Nanoscale

Accepted Manuscript

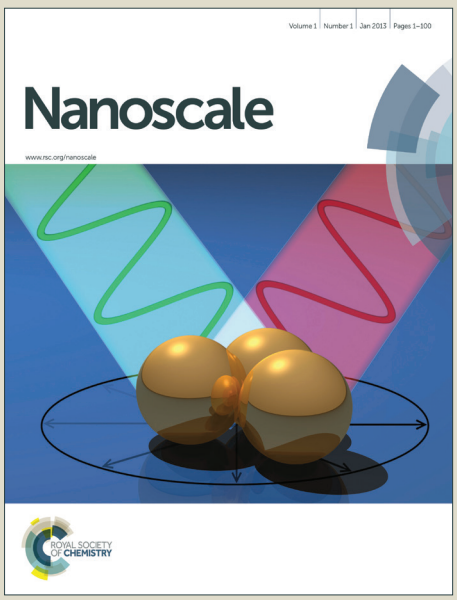

ROYAL SOCIETY OF CHEMISTRY

www.rsc.org/nanoscale

Nanoscale

COMMUNICATION

Large-scale freestanding nanometer-thick graphite pellicle for mass production of nanodevices beyond 10 nm

Received 00th January 20xx,
Accepted 00th January 20xx

DOI: 10.1039/x0xx00000x

www.rsc.org/nanoscale

Seul-Gi Kim,[†a] Dong-Wook Shin,[†a] Taesung Kim,[a] Sooyoung Kim,[a] Jung Hun Lee,[b] Chang Gu Lee,[a] Cheol-Woong Yang,[b] Sungjoo Lee,[a] Sang Jin Cho,[c] Hwan Chul Jeon,[d] Mun Ja Kim,*[d] Byung-Gook Kim,[d] and Ji-Beom Yoo*[ab]

Extreme ultraviolet lithography (EUVL) has received much attention in the semiconductor industry as a promising candidate to extend dimensional scaling beyond 10 nm. We present a new pellicle material, nanometer-thick graphite film (NGF), which shows an extreme ultraviolet (EUV) transmission of 92% at a thickness of 18 nm. The maximum temperature induced by laser irradiation (λ = 800 nm) of 9.9 W/cm^2 was 267 °C, due to the high thermal conductivity of the NGF. The freestanding NGF was found to be chemically stable during annealing at 500 °C in a hydrogen environment. A 50 × 50 mm large area freestanding NGF was fabricated using the wet and dry transfer method (WaDT). The NGF can be used as an EUVL pellicle for the mass production of nanodevices beyond 10 nm.

Extreme ultraviolet lithography (EUVL), at a wavelength of 13.5 nm, is an indispensable technique to extend dimensional scaling beyond 10 nm in the semiconductor industry.[1,2] For the high-volume manufacturing of Si-based nanodevices using extreme ultraviolet lithography (EUVL), controlling mask defectivity during the exposure to extreme ultraviolet (EUV) light has been considered the top priority among the various challenges, such as increasing the EUV source power and improving the line-width roughness of the resist.[3-5] Using a physical particle shield, a pellicle, complete blocking of the particle adders on the reflection mask during EUV exposure can be achieved, and it have been used in the imaging process of standard optical lithography for the same purpose.[6-8] However, issues of the pellicle materials are still remaining because of the strict requirements of EUVL pellicle.[6,9] For practical application to EUVL, a pellicle should have an EUV transmission of more than 90%, excellent thermal and chemical stability upon exposure to EUV with a high energy density of 5 W/cm^2 in a hydrogen environment, and large freestanding size of 110 × 140 mm.[6]

Based on these strict requirements of EUVL pellicles, freestanding thin films composed of several different materials, including Si, Ru, Mo, and Nb, have been investigated.[6,8,10] Among them, a 60-nm thick Si-based pellicle with a size of 110 × 140 mm showed the highest EUV transmission of ~85%.[6,9] However, it was crippled by the high temperature induced by EUV irradiation with a power density of 5 W/cm^2 due to the low thermal conductivity and reduced emissivity of the very thin Si layer.[6] This thermal breakdown of Si caused us to look for other material with high EUV transmission and thermal stability against EUV induced heating. Here, we present a new pellicle material, nanometer-thick graphite film (NGF), which has high theoretical EUV transmission,[11] heat dissipation properties,[12-14] and chemical stability.[15] NGF synthesized by chemical vapor deposition (CVD) shows an EUV transmission of 92% at a thickness of 18 nm, along with excellent chemical stability and heat dissipation properties. A 50 × 50 mm large-scale freestanding NGF pellicle was fabricated by the wet and dry transfer (WaDT) method. The EUV transmission, heat dissipation properties, and chemical stability of the NGF pellicle confirm the feasibility of using NGF pellicles for the mass production of nanodevices beyond 10 nm.

Since the EUV beam passes through the pellicle twice because of the reflection mask (Figure S1), the EUV transmission of a pellicle is directly related to the efficiency of EUV lithography. To obtain high transmission above 90%, NGFs with various thicknesses were synthesized by controlling the growth temperature in the range from 910 to 1035 °C. The thicknesses of the NGFs were measured using AFM and found to vary from 18 to 78 nm (Figure S2). Each freestanding NGF was fabricated on a circular frame with an inner diameter of 10 mm (inset in Figure 1a) by the scooping method and its transmission was measured at EUV (λ = 13.5 nm) and visible light (λ = 550 nm) wavelengths as shown in Figure 1a. The EUV transmission of the freestanding NGF with a thickness of 18 nm was

[a] SKKU Advanced Institute of Nanotechnology (SAINT) and center for Human Interface Nano Technolgy (HINT), Sungkyunkwan University, Suwon, 440-746, Republic of Korea.
[b] School of Advanced Materials Science and Engineering (BK21), Sungkyunkwan University, Suwon, 440-746, Republic of Korea.
[c] Fine Semitech, Osan, 447-210, Republic of Korea.
[d] Mask Development Team, Semiconductor R&D Center, SAMSUNG ELECTRONICS CO., Ltd, Hwaseong, 445-701, Republic of Korea.
† These authors contributed equally.
[§] Footnotes relating to the title and/or authors should appear here.
Electronic Supplementary Information (ESI) available: [details of any supplementary information available should be included here]. See DOI: 10.1039/x0xx00000x

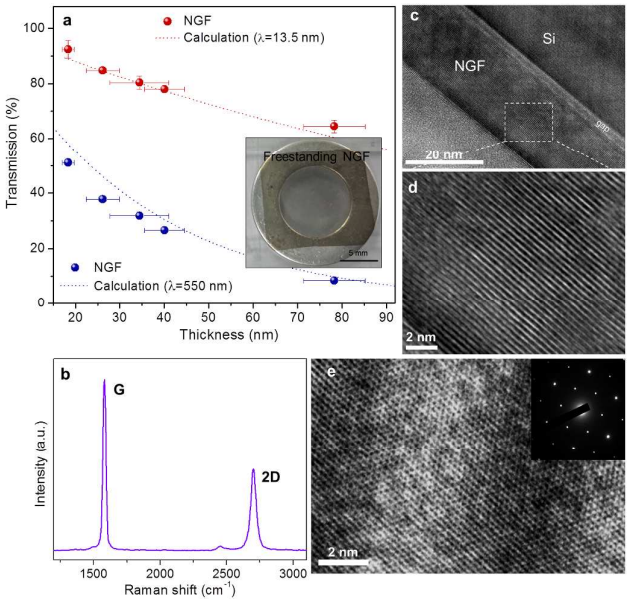

Fig. 1 Transmission of freestanding nanometer-thick graphite film (NGF), Raman spectrum of NGF, and high-resolution transmission electron microscopy (HRTEM) image. (a) EUV (λ = 13.5 nm) and visible light (λ = 550 nm) transmission of the NGF pellicle as a function of NGF thickness. The inset of (a) is a photo image of the pellicle (18 nm thick freestanding NGF) with a diameter of 10 mm. The red and blue dotted lines correspond to the simulations of transmission for EUV and visible light, respectively. (b) Representative Raman spectrum of NGF. (c) A cross-sectional TEM image of the thickness of 18 nm and (d) a well-arranged layer structure of the NGF. (e) HRTEM image of the NGF. The inset of (e) is the selected area electron diffraction (SAED) pattern of the NGF. The SAED pattern was collected using a 1.2 μm aperture.

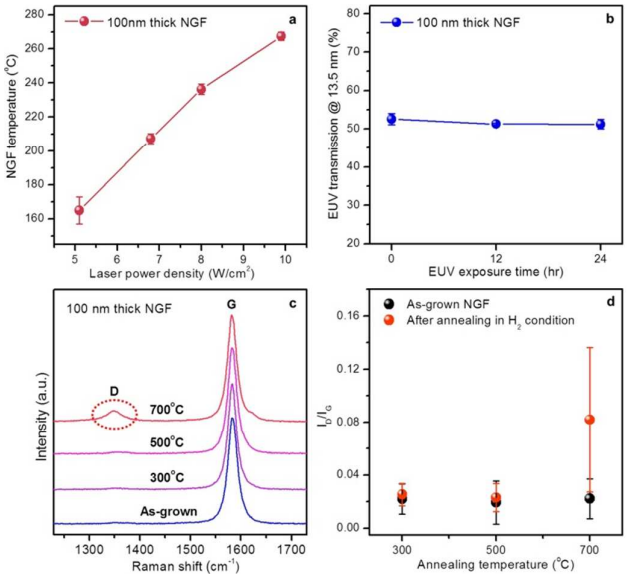

Fig. 2 Thermal and chemical stability of NGF in hydrogen and infrared (IR) laser irradiation environment. The thickness of the NGF was 100 nm and the inner diameter of the pellicle was 5.3 mm. (a) The maximum temperature of the freestanding NGF was measured by a thermal image camera as a function of the power density of the laser (λ = 800 nm). (b) The EUV transmission (λ = 13.5 nm) of the NGF with increasing exposure time in a hydrogen environment at a power density of 5 W/cm^2. The diameter of the laser beam was 4 mm and the chamber pressure in the hydrogen environment was 3 Pa. (c) Raman spectra of NGF after thermal annealing in hydrogen environment at various temperatures for 4 h. (d) I_D/I_G of NGF before and after annealing at different temperatures.

92% (51% @ 550 nm), which was the best EUV transmission among the EUV pellicles using Si and other thin films,[6,8,10] and represents excellent optical properties and shows the feasibility of NGF for EUV pellicles. The correlation between the transmission at the EUV and visible light wavelengths suggests a convenient way to assess the EUV transmission from visible light transmission. Theoretical calculations on the EUV and UV transmissions were carried out‡ based on the Beer-Lambert law. The simulation results of the EUV transmission (red dotted line) and visible light transmission (blue dotted line) with various thicknesses showed good agreement with the measured values.[11,16] The representative Raman spectrum of the NGF showed typical Raman spectra features of highly oriented pyrolytic graphite,[17] and the nanometer thickness of the graphite was confirmed by a cross sectional transmission electron microscopy (TEM) (Figure 1b and c). The thickness of the NGF was 18 nm and the well-arranged layer structure was observed (Figure 1d). The thicknesses of the NGFs synthesized at other temperatures were 28 nm (925 °C) and 67 nm (1000 °C), and the fine graphite structures were also observed without changes in the crystalline qualities (Figure S4). The high-resolution TEM (HRTEM) image of the NGF shown in Figure 1e reveals the uniform honeycomb structure of the NGF. The crystallinity of NGF was observed indirectly by the selected area electron diffraction pattern which was collected using a 1.2 μm aperture (Figure S4).

For the application of the freestanding NGF to EUV pellicles, its thermal and chemical stability should be ensured in an EUV lithography environment. We investigated the thermal and chemical stability of the NGFs using an infrared (IR, λ = 800 nm) laser and rapid thermal annealing (RTA) system. The IR laser was used as the heat source, because the absorption of the IR laser in NGF is higher than that of EUV (Supporting Information, Figure S3).[18] Considering that the EUV source power required for high-volume manufacturing is 250 W, corresponding to 5 W/cm^2 for the pellicle,[6] the power density of the IR laser beam should be higher than 5 W/cm^2. Figure 2a shows the maximum temperatures of the freestanding NGFs, induced by various power densities (higher than 5 W/cm^2) of the laser. The temperature, achieved instantly upon exposure to laser irradiation, was measured using a thermal imaging camera (Fluke, Ti10), and the pressure was maintained with a 3 Pa hydrogen environment. The maximum temperatures of 165 °C and 267 °C were measured at power densities of 5.1 W/cm^2 and 9.9 W/cm^2, respectively. The maximum temperature induced by the irradiation of the laser is very low compared with that of the Si-

based pellicle,[6] suggesting that it is an excellent heat dissipation material due to the high thermal conductivity.[12] The temperature profile of the NGF with a power density of 5.1 W/cm^2 is shown in Figure S5. The EUV transmission was not changed after 24 h of laser irradiation (Figure 2b). Raman spectra before and after irradiation also show almost the same intensity ratios of the D to G peaks (I_D/I_G), indicating that the levels of crystalline defect had not been changed (Figure S6). Figures 2c and d show the Raman spectra and I_D/I_G of the NGF after the chemical stability test using a RTA system in a hydrogen environment (3 Pa) at elevated temperatures for 4 h. The I_D/I_G of each Raman spectrum remained almost the same as that of the as-grown NGF up to 500 °C, except at 700 °C where the I_D/I_G changed from 0.02 to 0.08. The excellent heat dissipation properties and chemical stability show the feasibility of NGF in the EUV pellicle environment.

In addition to an EUV transmission of over 90% and stability in thermal and chemical environments, the scalability of the freestanding film size should be ensured for the application of the NGF to EUV pellicles. Figure 3a shows the scheme of the wet and dry transfer (WaDT) process for the fabrication of the large-scale freestanding NGF with a freestanding size of 50 × 50 mm. The

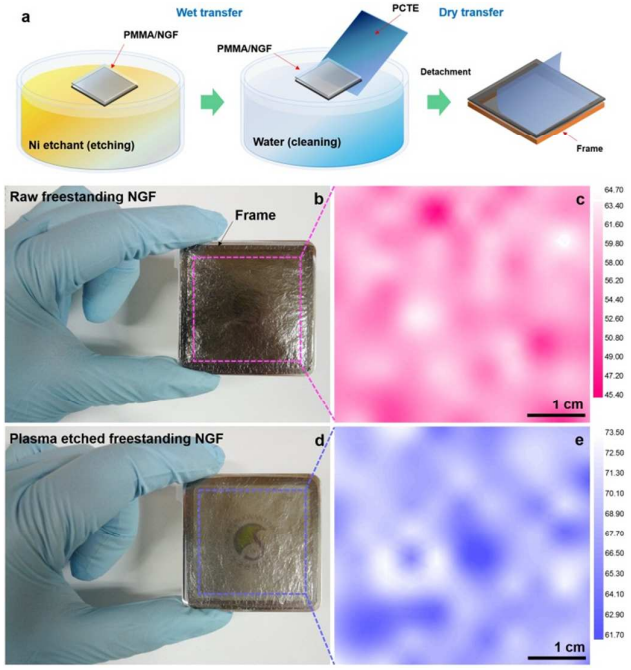

Fig. 3 Large-scale freestanding process, EUV transmission maps of NGF and their photo images. (a) Scheme of wet and dry transfer (WaDT) process for large-scale freestanding NGF. A PMMA-coated NGF was floated on water after Ni etching and washing. A polycarbonate track etched (PCTE) membrane was used for the wet transfer of NGF. A half-dried PMMA/NGF/PCTE was attached directly on the frame, and then a PCTE membrane was simply detached (dry transfer). (b,d) Photo images of the large-scale freestanding NGFs (50 × 50 mm) before and after O_2 plasma treatment. (c,d) EUV transmission maps (45 × 45 mm) before and after O_2 plasma etching.

fabrication procedure for the large-scale freestanding NGF is as follows: NGF coated with PMMA was floated on water and then transferred onto a polycarbonate track etched (PCTE) membrane. The half-dried PMMA/NGF/PCTE was attached directly onto a 50 × 50 mm frame with adhesive. Finally, the PCTE membrane was simply detached from the PMMA/NGF, and the PMMA was removed by oxygen plasma treatment (Supporting Information, Figure S7).[19,20] The product of the large-scale freestanding NGF (50 × 50 mm) is shown in Figure 3b. The thickness of the freestanding NGF was 86.06 ± 8.13 nm, which was obtained from EUV transmission map (57.59 ± 2.91 %, Figure 3c).[11] To obtain a high EUV transmission large-scale freestanding NGF, thickness of a NGF was reduced by oxygen plasma. As a function of etching time, the transmission of the NGF at visible light (λ = 550 nm) was measured with UV-vis-NIR spectrometer (Figure S8). The large-scale freestanding NGF having the thickness of 59.73 ± 5.83 nm was fabricated by applying this treatment condition, as shown in Figure 3d. The EUV transmission of the NGF is 68.17 ± 2.91 %. We found that the areal non-uniformity of EUV transmission might be induced by large wrinkles of freestanding NGF[6,21] formed in the NGF transfer processes conducting in ambient condition. Even though further studies are needed to get a uniform-transmission freestanding film, a large-scale freestanding NGF (or full-size NGF pellicles) with a high EUV transmission, above 90%, can be obtained by plasma treatment.

Conclusions

The excellent optical properties, high thermal stability, and the possibility of large scaling of the NGF demonstrate convincingly that NGF is the best material for the EUV pellicle. The EUV transmission of 92% on freestanding film (10 mm in diameter) and 50 × 50 mm freestanding NGF with 59.7 nm thickness is demonstrated. NGF shows exceptional heat dissipation properties under IR laser illumination with a power density of 9.9 W/cm^2 and excellent chemical stability at 500 °C in a hydrogen environment. The NGF is expected to be the best material for EUV pellicles, and we believe the use of NGFs in EUVL moves up the implementation of high volume manufacturing of nanoscale devices beyond 10 nm.

Acknowledgement

This study was supported by the Basic Science Research Program through the National Research Foundation of Korea (NRF) funded by the Ministry of Education, Science and Technology (2009-0083540) and Samsung Electronics Co. Ltd.

Notes and references

‡$T_{EUV} = e^{-4\pi\beta N \cdot d/\lambda}$, where $\beta = 6.9054 \times 10^{-3}$ at λ = 13.5 nm and N·d is the thickness of the NGF,[11] and $T_{vis} = e^{-4\pi\kappa t/\lambda}$, where κ = 1.3 at λ = 550 nm and t is the thickness of the NGF[16] (See Supporting Information)

1 C. Wagner, N. Harned, *Nature Photonics*, 2010, **4**, 24.

2 P. Naulleau, J. E. Bjorkholm, M. Chandhok, EUVL System Patterning Performance. In *EUV Lithography*, W. Bakshi, Ed.; SPIE press: Bellingham, WA, and Wiley: Hobokin, NJ, 2009; p 515.
3 G. Tallents, E. Wagenaars, G. Pert, *Nature Photonics*, 2010, **4**, 809.
4 S. Wurm, EUV Lithography. In *VLSI Technology, Systems and Application (VLSI-TSA)*, Proceedings of Technical Program-2014 International Symposium on, Hsinchu, China, Apr 28-30, 2014; IEEE, 2014.
5 H. Tsubaki, S. Tarutani, N. Inoue, H. Takizawa, T. Goto, *Proc. SPIE*, 2013, **8679**, 867905-1.
6 L. Scaccabarozzi, D. Smith, P. R. Diago, E. Casimiri, N. Dziomkina, H. Meijer, *Proc. SPIE*, 2013, **8679**, 867904.
7 O. Wood, EUV lithography: Approaching pilot production. Presented at the 2010 International Workshop on EUV Lithography, Maui, HI, June 21-25, 2010.
8 Y. A. Shroff, M. Goldstein, B. Rice, S. H. Lee, K. V. Ravi, D. Tanzil, *Proc. SPIE*, 2006, **6151**, 615104.
9 C. Zoldesi, K. Bal, B. Blum, G. Bock, D. Brouns, F. Dhalluin, N. Dziomkina, J. D. Arias Espinoza, J. Hoogh, S. Houweling, M. Jansen, M. Kamali, A. Kempa, R. Kox, R. Kruif, J. Lima, Y. Liu, H. Meijer, H. Meiling, I. Mil, M. Reijnen, L. Scaccabarozzi, D. Smith, B. Verbrugge, L. Winter, X. Xiong, J. Zimmerman, *Proc. SPIE*, 2014, **9048**, 90481N-1.
10 Y. A. Shroff, M. Leeson, P.-Y. Yan, E. Gullikson, F. Salmassi, *J. Vac. Sci. Technol. B*, 2010, **28**, C6E36.
11 B. L. Henke, E. M. Gullikson, J. C. Davis, *Atomic Data and Nuclear Data Tables*, 1993, **54**, 181.
12 A. A. Balandin, *Nature Materials*, 2011, **10**, 569.
13 G. Neuer, *Int. J. Thermophys.*, 1995**, 16**, 257.
14 M. Freitag, M. Steiner, Y. Martin, V. Perebeinos, Z. Chen, J. C. Tsang, P. Avouris, *Nano Lett.*, 2009, **9**, 1883.
15 Y. H. Kahng, S. Lee, W. Park, G. Jo, M. Choe, J.-H. Lee, H. Yu, T. Lee, K. Lee, *Nanotechnology*, 2012**, 23**, 075702.
16 P. Blake, E. W. Hill, A. H. Castro Neto, K. S. Novoselov, D. Jiang, R. Yang, T. J. Booth, A. K. Geim, *Appl. Phys. Lett.*, 2007, **91**, 063124.
17 R. J. Nemanich, S. A. Solin, *Phys. Rev. B*, 1979, **20**, 392.
18 A. B. Djurišić, E. H. Li, *J. Appl. Phy.*, 1999, **85**, 7404.
19 K. Kumar, Y.-S. Kim, E.-H. Yang, *Carbon*, 2013, **65**, 35.
20 G. Xie, R. Yang, P. Chen, J. Zhang, X. Tian, S. Wu, J. Zhao, M. Cheng, W. Yang, D. Wang, C. He, X. Bai, D. Shi, G. Zhang, *Small*, 2014, **10**, 2280.
21 J. B. Kim, P. Kim, N. C. Pégard, S. J. Oh, C. R. Kagan, J. W. Fleischer, H. A. Stone, Y.-L. Loo, *Nature Photonics*, 2012, **6**, 327.

Supporting Information for

Large-Scale Freestanding Nanometer-thick Graphite Pellicle for Mass Production of Nanodevices beyond 10 nm

Seul-Gi Kim, Dong-Wook Shin, Taesung Kim, Sooyoung Kim, Jung Hun Lee, Chang Gu Lee, Cheol-Woong Yang, Sungjoo Lee, Sang Jin Cho, Hwan Chul Jeon, Mun Ja Kim★, Byung-Gook Kim, and Ji-Beom Yoo★

★Corresponding author. E-mail: jbyoo@skku.edu (J.-B.Y.); munja.kim@samsung.com (M.J.K.)

1. Transmission and absorption of NGF at EUV (λ = 13.5 nm), visible (λ = 550 nm), and IR (λ = 800 nm) wavelengths

For EUV, the transmission of the NGF can be expressed in terms of the optical constant for the EUV regime $\beta \approx (r_0 \cdot \lambda^2/2\pi) n_c f_{2c}(0)$, as $T_{EUV} = e^{-4\pi\beta N.d/\lambda}$ where $N \cdot d$ is thickness of the film, λ is wavelength of the EUV, r_0 is classical electron radius, n_c is atomic density of NGF, and $f_{2c}(0)$ is the imaginary part of the atomic scattering factor of carbon at normal incident angle[11]. For visible light, transmission can be expressed as $T = e^{-4\pi\kappa t/\lambda}$ where $\kappa = 1.3$ is the extinction coefficient of graphite at $\lambda = 550$ nm, and t is the thickness of the NGF.

Absorption of light in a material can be expressed as $A = 1 - T - R$, where A is absorption, T is transmission, and R is reflection. With 100-nm-thick NGF, an EUV transmission at 13.5 nm can be calculated with T_{EUV} and β, and the value is 52.6%. Reflectance is not considered because of the very small value. Thus, the absorption of the NGF at the EUV wavelength is 47.4%. At the IR wavelength (800 nm), the transmission

equation is almost the same as that of visible light except the value of κ. κ = 1.7 is introduced and the transmission at a wavelength of 800 nm is 6.9%. Reflectance can be expressed as $R = ((n - n_0)^2 + \kappa^2)/((n + n_0)^2 + \kappa^2)$ and is 36.5%, where $n_0 = 1$ is the refractive index of vacuum and n = 3.0 and κ = 1.7 are the real and imaginary parts of the complex refractive index of the NGF[18]. So, the calculated absorption of the NGF with the thickness of 100 nm is 56.6%. This is very close to the measured value of absorption of NGF, 57.1% (Figure S3).

2. Removal of PMMA by oxygen plasma treatment

A PMMA layer in the scooping and wet and dry transfer (WaDT) methods was used as a support layer for stable transfer of NGF on the frame. Generally, PMMA was removed by thermal annealing and solvent rinses[19]. Although these methods are useful in the case of NGF transfer onto flat substrates, in cases of large-scale freestanding NGF, the sagging problem and the destruction of NGF by thermal annealing and/or surface tension between NGF and solvent were observed. Thus, we used the method of oxygen plasma treatment to remove the PMMA for large-scale freestanding NGFs. The pressure of oxygen was ~ 0.38 Torr, and plasma with a radio frequency of 13.6 MHz and power of 50 W was used. Large-scale freestanding NGFs were treated for 5 min. Figure S7 shows the optical images of as-grown NGF, PMMA/NGF, NGF treated by plasma for 2 min, and 5 min. After oxygen plasma treatment for 5 min, PMMA was completely removed from NGF.

3. Control of NGF thickness by oxygen plasma treatment

NGF synthesized at 1000 °C was coated with PMMA layer, and then it was transferred on a 20 × 20 mm frame by WaDT method after Ni etching and cleaning. The conditions for the oxygen plasma were the same as that for the removal of PMMA. After the removal of PMMA layer on NGF by oxygen plasma treatment for 5 min, NGF was treated by plasma for additional 5 min to 80 min. Figure S8 shows the variation of the transmission of NGF at the visible wavelength of 550 nm as a function of oxygen plasma treatment time and the photo images of NGF/PMMA and NGF treated by oxygen plasma. Thickness of NGF was calculated by Beer-Lambert law (See chapter 2 about transmission and absorption of NGF). As plasma treatment time was increased, thickness of NGF was decreased. The etching rate of NGF by oxygen plasma was ~0.226 nm/min. For 80 min of plasma treatment, the transmission of NGF is enhanced by 9%, and thickness of NGF is reduced by 18.7 nm. The photo image of NGF after oxygen plasma treatment (Figure S8D) is more transparent than that of NGF before treatment (Figure S8C). Graphene (or multi-layered graphene) was generally damaged after oxygen plasma treatment[20]. So, we evaluated the plasma-induced defects of NGF by Raman spectroscopy. Generally, our NGF shows ~0.02 of I_D/I_G in Raman spectroscopy. After removal of PMMA from PMMA/NGF by plasma treatment for 5 min, I_D/I_G was increased from ~0.022 to ~0.053. After 80 min, I_D/I_G was increased to ~0.134, as shown in Figure S8B.

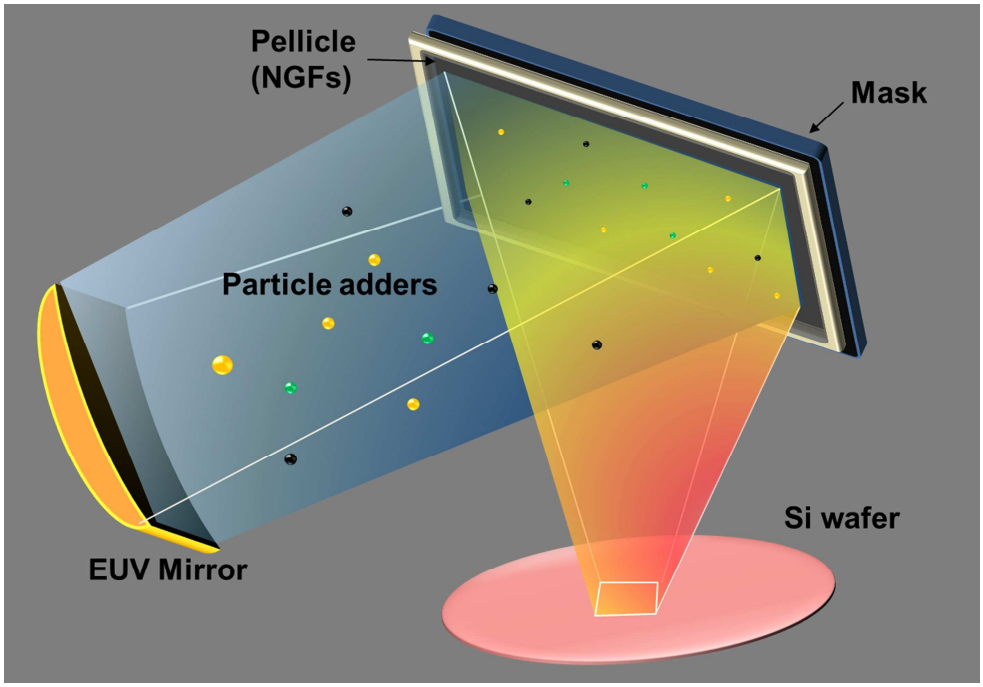

Figure S1. Scheme of EUV lithography. An EUV beam generated from an EUV source is reflected via an EUV mirror and goes through the pellicle twice by a reflection mask. Energy efficiency transferred onto Si wafer that directly affects production efficiency is proportional to the square of the pellicle transmission, and thus improvement of EUV transmission of the EUVL pellicle is required.

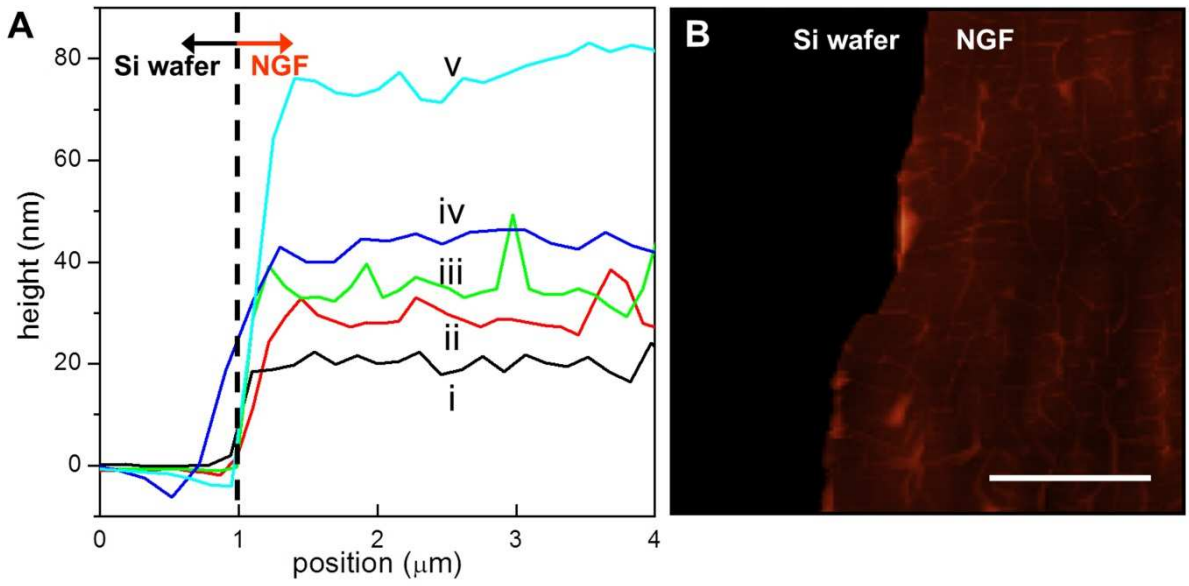

Figure S2. Thickness of nanometer-thick graphite film (NGF) measured by AFM. (A) AFM line profiles obtained at the edge of the NGF from 18 nm (i) to 78 nm (v). Each thickness was obtained after transfer of the NGF on to a Si wafer. (B) Typical AFM topographic image of NGF (34 nm thick). The scale bar of (B) is 5 μm.

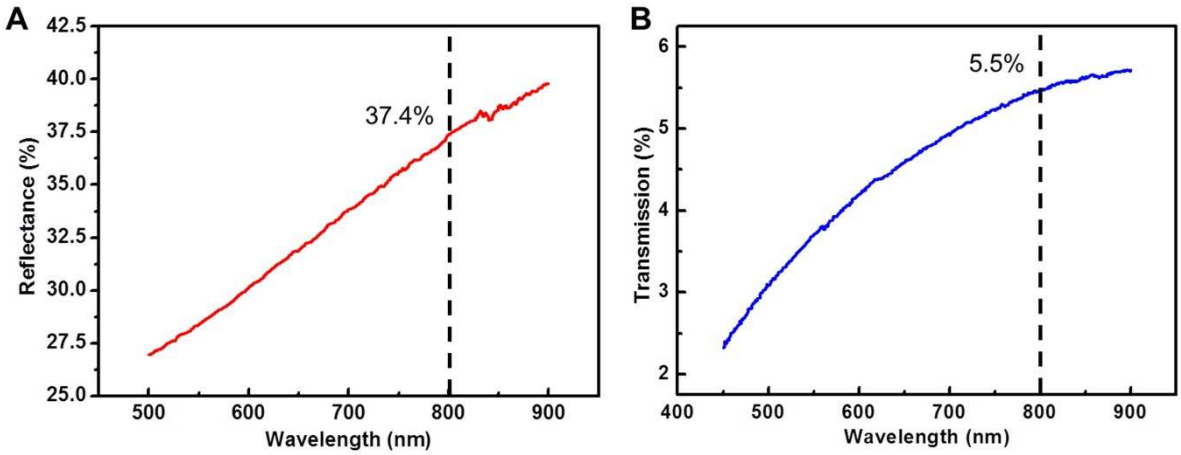

Figure S3. Reflectance and transmission of the 100 nm thick NGF measured by UV-vis NIR spectrometer. (A) Reflectance and (B) transmission of the NGF to the incident light were measured as 37.4% and 5.5%, respectively. At a wavelength of 800 nm, 57.1% of the incident laser power was absorbed and converted into heat in NGF.

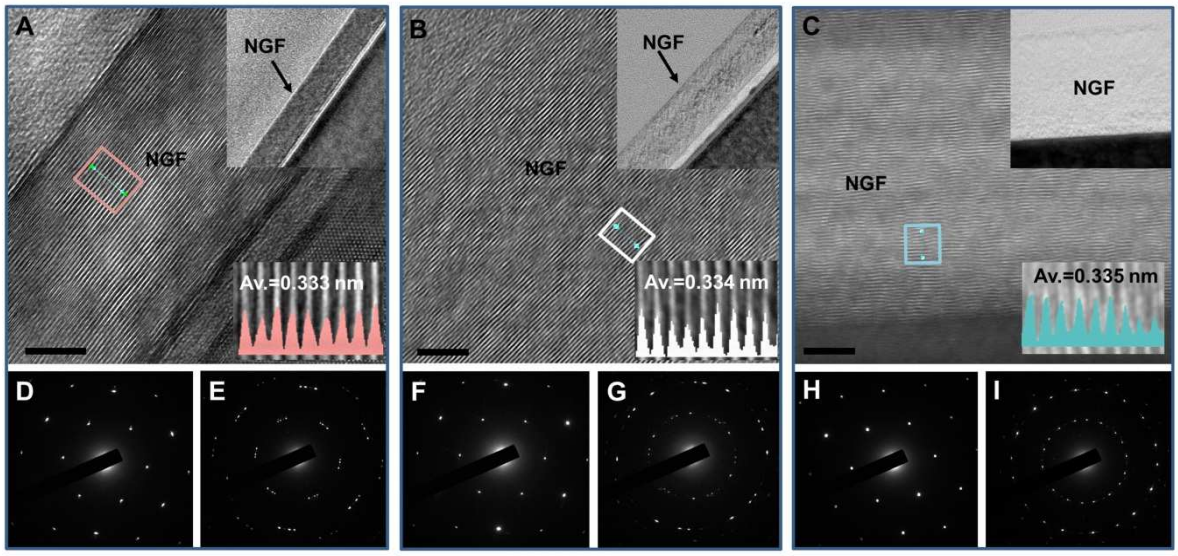

Figure S4. TEM cross-section image and electron diffraction pattern of NGFs. (A-C) High-resolution TEM cross-section images of the NGFs of various thicknesses. The thicknesses of NGF synthesized at 910, 925, and 1000 °C were 18, 28, and 67 nm, respectively. The top-right inset of (A-C) show the cross-sectional view of each film. The bottom-right inset of (A-C) show the magnified image of the marked area in (A-C) and the layer distance from the intensity profile. They are very close to theoretical layer distance of the graphite, 0.335 nm, and show a well-arranged layer structure. (D-I) The selected area electron diffraction (SAED) patterns of (A-C). Each NGF has similar SAED patterns: (i) well-defined hexagonal and (ii) hexagonal patterns by overlapped grain, indicating the polycrystalline structure of the NGFs. Each SAED pattern was collected using a 1.2 μm aperture. The scale bar is 5 nm.

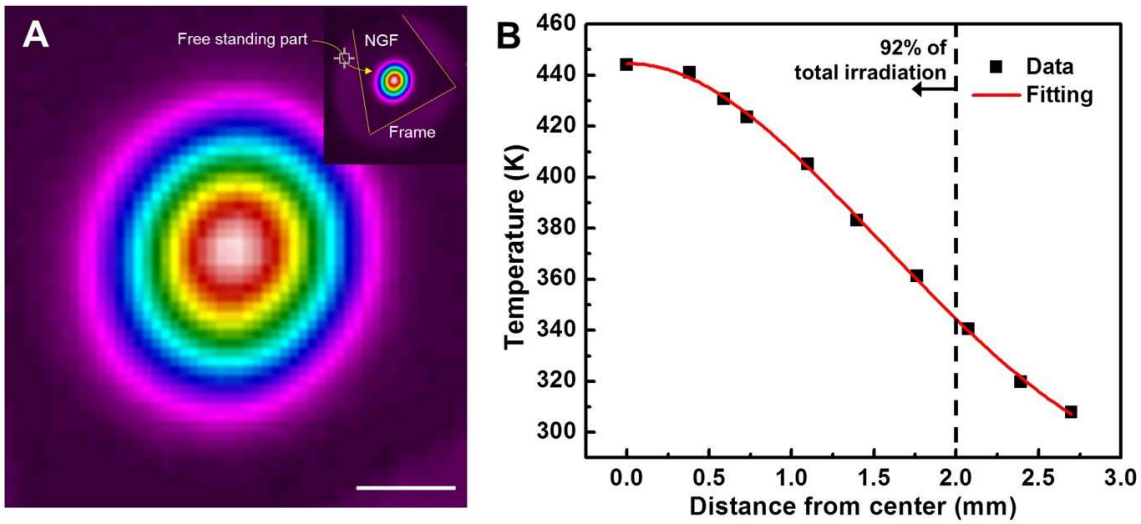

Figure S5. Temperature profile of NGF with IR laser irradiation. (A) The thermal image of the NGF pellicle with 5.1 W/cm^2 of IR laser irradiation, and (B) temperature profile. The scale bar of (A) is 2 mm. The inner diameter of the free-standing pellicle was 5.3 mm and outer diameter of the frame was 12.0 mm. An IR laser with a wavelength of 800 nm was illuminated onto the center of the pellicle. About 92% of total intensity of the incident beam was focused within 2 mm from the center of the beam. Temperatures profile of the NGF was obtained from the analysis of thermal image, and the temperature profile (Figure S5B) was fitted using polynomials.

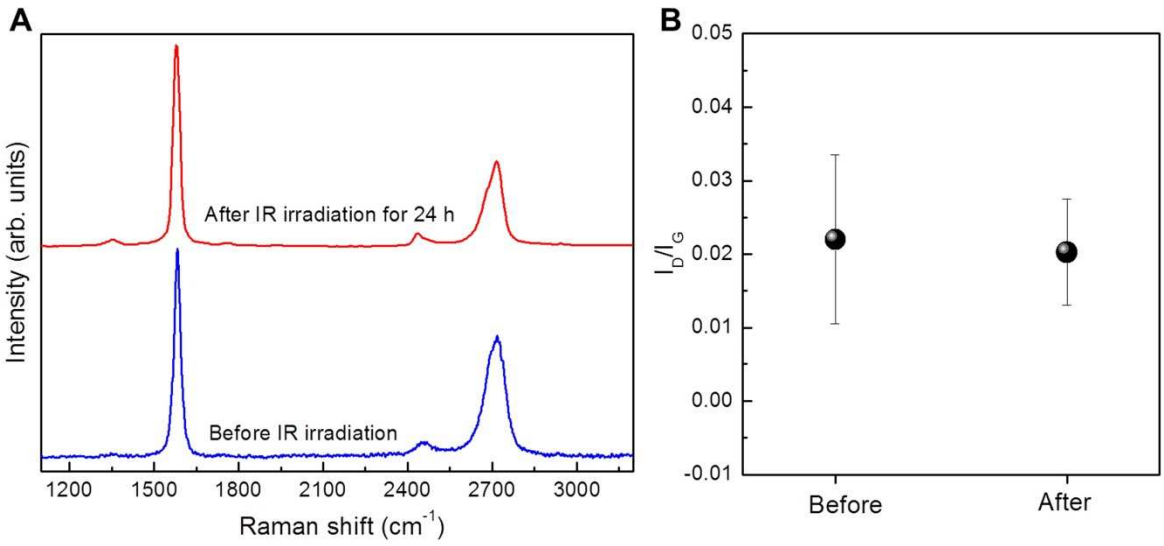

Figure S6. Raman spectra of the NGF pellicle before and after IR laser irradiation.

(A) Raman spectra of the freestanding NGF pellicle before and after IR laser irradiation.

(B) No enhancement of the D-band was observed after IR irradiation.

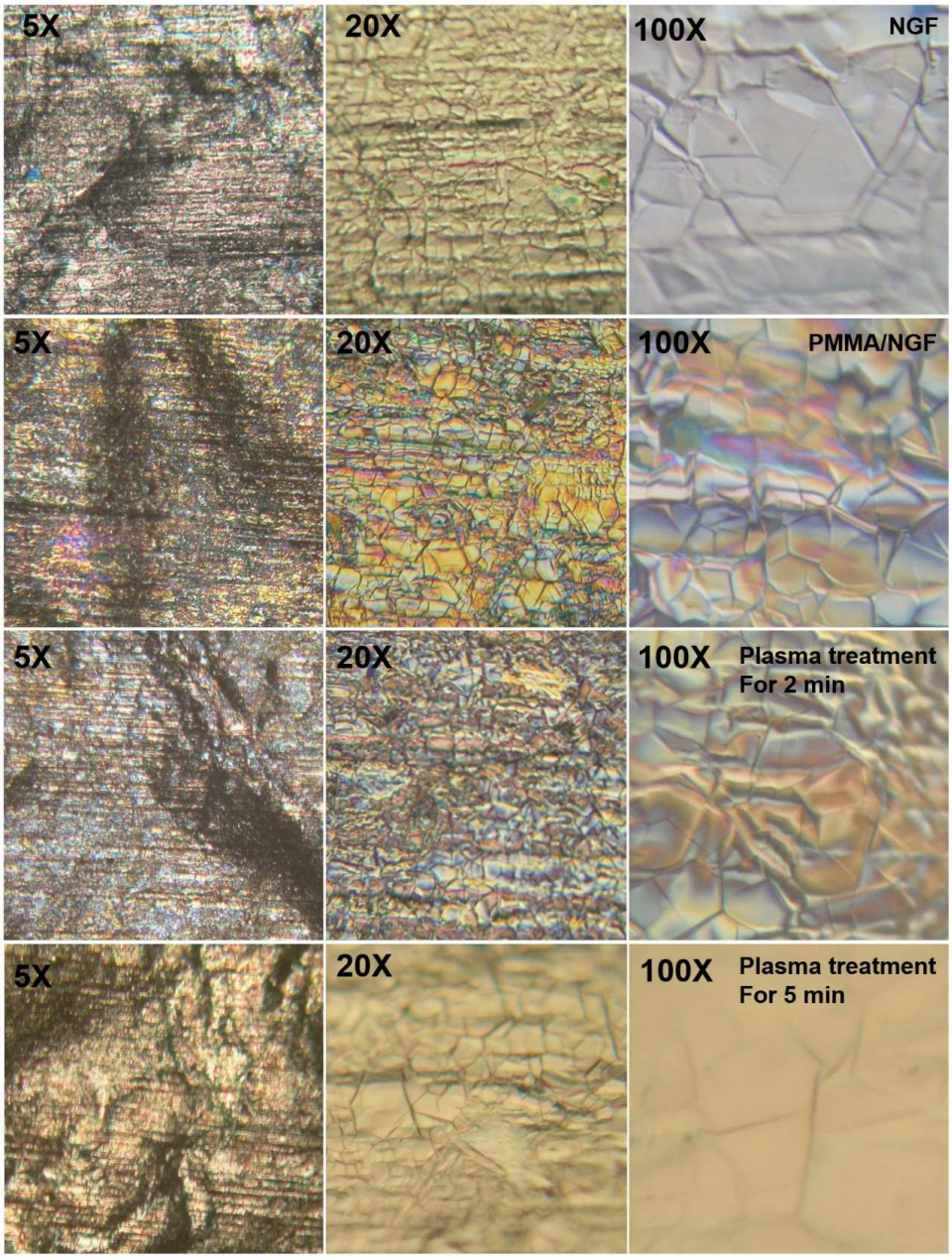

Figure S7. Optical images of NGFs and PMMA/NGFs before and after O_2 plasma treatment. After oxygen plasma treatment for 5 min, PMMA was completely removed from NGF. The pressure of oxygen was ~ 0.38 Torr, and plasma with a radio frequency of 13.6 MHz and power of 50 W was used.

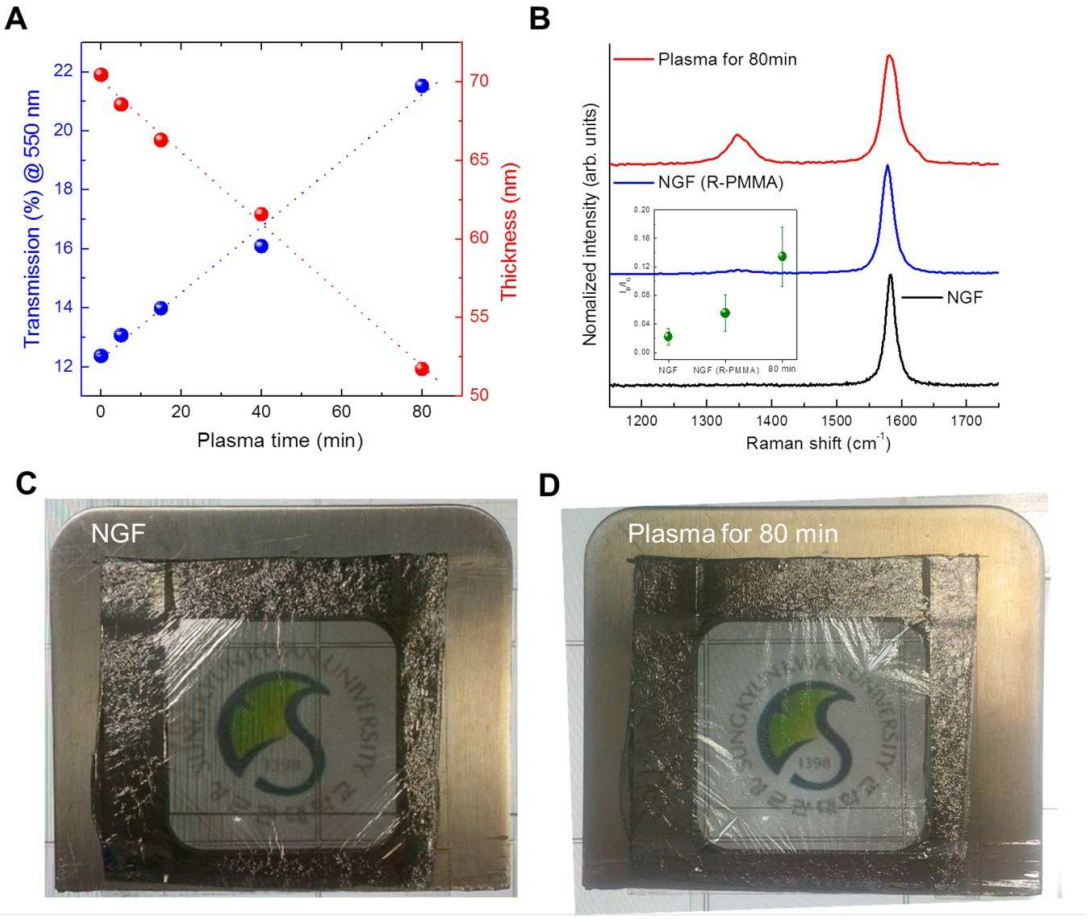

Figure S8. Control of NGF thickness by oxygen plasma treatment (20 × 20 mm frame). (A) Variation of the transmission of NGF and calculated thickness at visible wavelength of 550 nm as a function of oxygen plasma treatment time. Thickness of NGF was calculated by Beer-Lambert law (See chapter 2). For 80 min of etching time, the transmission of NGF was enhanced by 9% and the thickness of the NGF was reduced by 18.7 nm. (B) Raman spectra of NGF, NGF (R-PMMA) (PMMA removed from NGF), and NGF treated by plasma for 80 min, and (C-D) the photo images of NGF (after removal of PMMA) and NGF treated by oxygen plasma for 80 min. The inset of (B) is I_D/I_G ratio of each film.